Second-order all-fiber comb filter based on polarization-diversity loop configuration

Yong Wook Lee[1*], Hyun-Tak Kim[2], and Yong Wan Lee[3]

[1]*School of Electrical and Control Engineering, Pukyong National University, Busan 608-739, Korea*
[2]*IT Components & Material Research Division, Electronics and Telecommunications Research Institute, 161 Gajeong-Dong, Yuseong-Gu, Daejeon 305-350, Korea*
[3]*Department of Electrical and Computer Engineering, University of Minnesota, Minneapolis, MN 55455, USA*
**Corresponding author: yongwook@pknu.ac.kr*

Abstract: By concatenating three birefringence loops in series, a second-order all-fiber comb filter based on a polarization-diversity loop configuration is newly proposed. The proposed filter consists of one polarization beam splitter, polarization-maintaining fibers, and two half-wave plates. The effect of a second-order structure of polarization-maintaining fiber loops on a bandwidth of the filter passband was theoretically analyzed and experimentally demonstrated. Transmission output of the second-order filter (flat-top and narrow-band transmission spectra) could be obtained by adjusting two half-wave plates. 1 and 3 dB bandwidths of the proposed filter in flat-top and narrow-band operations were greater by ~102.9 and 44.3 % and smaller by ~47.9 and 47.1 % than those of a conventional Sagnac birefringence filter, respectively.

OCIS codes: (350.2460) Filters, interference; (060.2420) Fibers, polarization-maintaining; (060.2330) Fiber optics communications.

References and links

1. X. Fang and R. O. Claus, "Polarization-independent all-fiber wavelength-division multiplexer based on a Sagnac interferometer," Opt. Lett. **20**, 2146-2148 (1995).
2. Y. W. Lee, J. Jung, and B. Lee, "Multiwavelength-switchable SOA-fiber ring laser based on polarization-maintaining fiber loop mirror and polarization beam splitter," IEEE Photon. Technol. Lett. **16**, 54-56 (2004).
3. M. P. Fok, K. L. Lee, and C. Shu, "Waveband-switchable SOA ring laser constructed with a phase modulator loop mirror filter," IEEE Photon. Technol. Lett. **17**, 1393-1395 (2005).
4. X. Fang, K. Demarest, H. Ji, C. T. Allen, and L. Pelz, "A subnanosecond polarization-independent tunable filter/wavelength router using a Sagnac interferometer," IEEE Photon. Technol. Lett. **9**, 1490-1492 (1997).
5. G. Zhu, Q. Wang, H. Chen, H. Dong, and N. K. Dutta, "High-quality optical pulse train generation at 80 Gb/s using a modified regenerative-type mode-locked fiber laser," IEEE J. Quantum Electron. **40**, 721-725 (2004).
6. G. Rossi, O. Jerphagnon, B.-E. Olsson, and D. J. Blumenthal, "Optical SCM data extraction using a fiber-loop mirror for WDM network systems," IEEE Photon. Technol. Lett. **12**, 897-899 (2000).
7. X. Fang, H. Ji, C. T. Allen, K. Demarest, and L. Pelz, "A compound high-order polarization-independent birefringence filter using Sagnac interferometers," IEEE Photon. Technol. Lett. **9**, 458-460 (1997).
8. Z. Jia, M. Chen, and S. Xie, "Label erasing technique employing Lyot-Sagnac filter," Electron. Lett. **38**, 1563-1564 (2002).
9. Y. W. Lee, H.-T. Kim, J. Jung, and B. Lee, "Wavelength-switchable flat-top fiber comb filter based on a Solc type birefringence combination," Opt. Express **13**, 1039-1048 (2005).
10. I. Solc, "Birefringent chain filters," J. Opt. Soc. Am. **55**, 621-625 (1965).
11. R. C. Jones, "New calculus for the treatment of optical systems," J. Opt. Soc. Am. **31**, 488-492 (1941).
12. Y. Shiquan, L. Zhaohui, D. Xiaoyi, Y. Shuzhong, K. Guiyun, and Z. Qida, "Generation of wavelength-switched optical pulse from a fiber ring laser with an F-P semiconductor modulator and a HiBi fiber loop mirror," IEEE Photon. Technol. Lett. **14**, 774-776 (2002).
13. P. Humphrey and J. E. Bowers, "Fiber-birefringence tuning technique for an erbium-doped fiber ring laser," IEEE Photon. Technol. Lett. **5**, 32-34 (1993).

#88023 - $15.00 USD Received 28 Sep 2007; revised 25 Dec 2007; accepted 26 Dec 2007; published 10 Mar 2008

1. Introduction

Owing to their simple design and ease of use, all-fiber comb filters based on a Sagnac birefringence loop (Sagnac birefringence filter: SBF) [1] have obtained much attention and have been usefully incorporated for development of multiwavelength fiber lasers [2,3], high-speed wavelength routing [4], optical pulse train generation [5], all-optical label swapping [6], etc. For obtaining various intensity transfer functions in the SBF, birefringence configurations (BC's) derived from conventional Solc and Lyot filters have been introduced into the Sagnac birefringence loop of the filter using polarization-maintaining fibers (PMF's) [7,8]. In previously reported flat-top SBF's [7,8], however, an inherent insertion loss was observed in the calculated transmission [7] and experimentally measured insertion loss seemed to be slightly high [8]. Recently, a polarization-independent first-order fiber comb filter has been reported on the basis of a Solc type BC and polarization-diversity loop configuration (PDLC), which could produce the flat-top and narrow-band transmission spectra without the inherent insertion loss mentioned above [9]. In this paper a polarization-independent second-order all-fiber comb filter based on the PDLC, which can make a passband much broader (or narrower), in addition to merit of no inherent insertion loss, compared with that of the previous first-order PDLC-based filter, is newly proposed by concatenating three birefringence loops in series. The proposed filter consists of one polarization beam splitter (PBS), three sections of polarization-maintaining fibers (PMF's) concatenated with a 30˚ angle offset among their adjacent principal axes, and two half-wave plates (HWP's). The effect of a second-order structure of PMF loops on the bandwidth of the filter passband was theoretically investigated and experimentally demonstrated.

2. Principles of operation

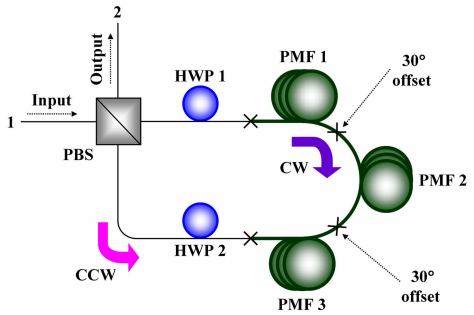

(a)

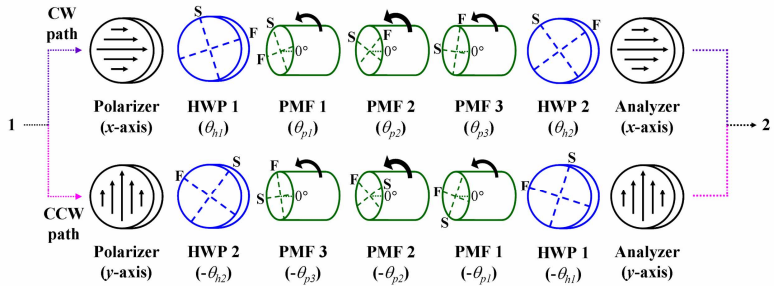

(b)

Fig. 1. (a) Schematic diagram of the proposed filter and (b) propagating light path when the input light transmits through the output port.

Figure 1(a) shows a schematic diagram of the proposed PDLC-based comb filter that consists of a PBS, two HWP's (HWP 1 and 2), and three PMF sections with the same length. Based on the Solc type BC [10], three PMF sections were concatenated with the 30˚ angle offset among

#88023 - $15.00 USD Received 28 Sep 2007; revised 25 Dec 2007; accepted 26 Dec 2007; published 10 Mar 2008

their adjacent principal axes. For simplicity, let us assume that horizontal and vertical axes of the PBS are designated as *x* and *y*-axes, respectively. First, let us also assume that the light introduced into the port 1 of the filter is *x*-polarized light (*x* polarization). Then, as shown in a clockwise (CW) path of Fig. 1(b), the input light propagates through the polarizer (*x*-polarized), HWP 1 (with its fast axis θ_{h1} oriented with respect to *x*-axis), PMF 1 (θ_{p1} oriented), PMF 2 ($\theta_{p2} = \theta_{p1} + 30°$ oriented), PMF 3 ($\theta_{p3} = \theta_{p1} + 60°$ oriented), HWP 2 (θ_{h2} oriented), and analyzer (*x*-polarized) sequentially, rotating in a CW direction. In Fig. 1(b), F and S indicate fast and slow axes of the PMF and HWP, respectively. The angle offset (30°) between principal axes of two adjacent PMF's (the PMF 1 and 2 or the PMF 2 and 3) was determined from an equation $\theta = \pi/4N$, that is, $2\theta = 2 \times \pi/12 = \pi/6$ rad ($N = 3$) [10].

In this filter structure, on the one hand, if two orientation angles of the HWP 1 and 2 are adjusted to effectively rotate the polarizer and analyzer by ($\theta_{p1} - 15°$) and ($\theta_{p1} + 75°$) with respect to *x*-axis, respectively, it is possible to make the geometrical arrangement of the polarizer, three PMF's, and analyzer form that of the fan Solc filter with three BP's and the 90° rotated analyzer [10], which gives the second-order flat-top transmission spectrum. On the other hand, if the polarizer and analyzer is effectively rotated, respectively, by ($\theta_{p1} - 105°$) and ($\theta_{p1} + 75°$) with respect to *x*-axis through the proper adjustment of the HWP's, it is also possible to make the geometrical arrangement of the optical components build that of the fan Solc filter with three BP's [10], which gives the second-order narrow-band transmission spectrum whose free spectral range is shifted by half a period.

Similarly, when the input light is *y*-polarized, the light travels the filter in a counterclockwise (CCW) direction as shown in a CCW path of Fig. 1(b). Due to the reversed sequence and *y*-axis symmetry of the optical components in the CCW direction, the same geometrical arrangement can be obtained as the case of the *x*-polarized input light. Especially, as an arbitrarily polarized light can always be decomposed into *x* and *y*-polarized components, the transmitted intensity becomes the superposition of intensity outputs of two interference spectra due to *x* and *y* input polarizations, and the transmitted output of the filter becomes independent of the input polarization. Consequently, the Solc type combination of three PMF sections in the proposed filter can produce much flatter or narrower passband in the output transmission spectra than the previous first-order PDLC-based filter can, that is, higher-order filter output can be achieved by simply adjusting the HWP's within the fiber loop of the filter.

The above discussion can be supported using Jones calculus [11]. Considering both CW and CCW paths, the Jones transfer matrix T and transmittance t_{filter} of the proposed filter are expressed as follows;

$$\begin{aligned} T = &\begin{bmatrix}1 & 0\\ 0 & 0\end{bmatrix} T_{H2}(\theta_{h2}) T_{P3}(\theta_{p3}) T_{P2}(\theta_{p2}) T_{P1}(\theta_{p1}) T_{H1}(\theta_{h1}) \begin{bmatrix}1 & 0\\ 0 & 0\end{bmatrix} \text{ (CW)} \\ &+ \begin{bmatrix}0 & 0\\ 0 & 1\end{bmatrix} T_{H1}(-\theta_{h1}) T_{P1}(-\theta_{p1}) T_{P2}(-\theta_{p2}) T_{P3}(-\theta_{p3}) T_{H2}(-\theta_{h2}) \begin{bmatrix}0 & 0\\ 0 & 1\end{bmatrix} \text{ (CCW)} \end{aligned} \tag{1}$$

$$\begin{aligned} t_{filter} = &\frac{9}{8}\left[\cos(2\theta_{h1} - 2\theta_{h2} + \frac{\pi}{3})\cos\Gamma + \frac{1}{6}\cos(2\theta_{h1} - 2\theta_{h2}) + \frac{\sqrt{3}}{2}\sin(2\theta_{h1} - 2\theta_{h2})\right]^2 \\ &\times(1+\cos\Gamma) + \frac{9}{8}\left[\cos(2\theta_{h1} + 2\theta_{h2} - 60^\circ - 2\theta_{p1})\left(\cos\Gamma + \frac{1}{3}\right)\right]^2 (1-\cos\Gamma) \end{aligned} \tag{2}$$

where T_{H1}, T_{H2}, T_{P1}, T_{P2}, and T_{P3} are Jones matrices of the HWP 1, HWP 2, PMF 1, PMF 2, and PMF 3, respectively. Γ ($= 2\pi BL/\lambda$) that is generated due to birefringence B and length L of one PMF (λ is the wavelength in vacuum) is a phase retardation difference between two orthogonally polarized modes. In the formulation, any insertion loss due to optical components was not considered, and the phase retardation difference of the HWP's was assumed wavelength-independent.

#88023 - $15.00 USD Received 28 Sep 2007; revised 25 Dec 2007; accepted 26 Dec 2007; published 10 Mar 2008

If [θ_{h1}, θ_{h2}] (orientation angles of the HWP 1 and 2) are selected to orient the polarizer and analyzer at the effective angles of (θ_{p1} – 15°) and (θ_{p1} + 75°) with respect to *x*-axis (e.g. [$\theta_{p1}/2 - \pi/24$, $\theta_{p1}/2 + 5\pi/24$]), respectively, the filter transmittance is given by {1– [1 + 7cosΓ + 15cos^{2}Γ + 9cos^{3}Γ]/32} (flat-top transmission spectrum). Similarly, if [θ_{h1}, θ_{h2}] is selected to orient the polarizer and analyzer, respectively, at the effective angles of (θ_{p1} – 105°) and (θ_{p1} + 75°) (e.g. [$\theta_{p1}/2 - 7\pi/24$, $\theta_{p1}/2 + 5\pi/24$]), the filter transmittance is given by {[1 + 7cosΓ + 15cos^{2}Γ + 9cos^{3}Γ]/32} (narrow-band transmission spectrum). In particular, orientation angles of HWP's, θ_{h1} and θ_{h2}, have an angle symmetry of π/2 in Eq. (2) because the HWP has the intrinsic angle symmetry of π in its azimuth angle. Figure 2 shows the transmission spectra of the proposed filter, which are based on the above calculated transmittances, plotted at two HWP combinations selected for the second-order filter operation: Flat-top and narrow-band transmission spectra are plotted in blue and red solid lines, respectively, and they have an interleaved (complementary) relationship with each other. In Fig. 2, the birefringence and length of the PMF were determined considering the phase retardation difference Γ so that the wavelength spacing between passband (channel) centers in the transmission spectrum could be 1.368 nm for further comparison with measured spectra of Fig. 3.

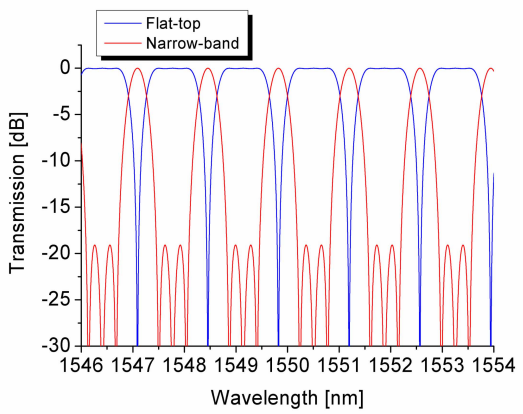

Fig. 2. Calculated flat-top (blue line) and narrow-band (red line) transmission spectra of the proposed filter.

3. Experiments and discussion

In order to examine the theoretical results, the proposed filter was implemented by using a Panda type PMF (Fibercore), a PBS (OZ Optics), and two HWP's (OZ Optics) as shown in Fig. 1(a). The birefringent section within the filter was composed of three PMF loops that were concatenated in series while the principal axes of two adjacent PMF loops had the 30° angle offset. The birefringence of the PMF was ~3.98×10^{-4}, and the lengths of three PMF loops (PMF 1, PMF 2, and PMF 3) were 4.41 m, 4.42 m, and 4.41 m, respectively. Splicing points between the PMF and single-mode fiber (SMF) or two PMF's were marked with crosses (X's) in the figure.

Figure 3 shows the flat-top (blue solid line) and narrow-band (red solid line) transmission spectra of the proposed filter measured at optimal angle sets of θ_{h1} and θ_{h2} ([θ_{h1}:θ_{h2}] = [65.5°:109.5°] and [20.5°:109.5°], respectively). As predicted in the theoretical results, the transmission output peculiar to the second-order filter (flat-top and narrow-band transmission spectra) can be obtained by the proper adjustment of two HWP's, and the flat-top transmission output has the complementary relationship to the narrow-band one. The wavelength spacing (channel spacing) between transmission minima of the filter spectrum was measured as ~1.37 nm, and the spectral flatness of one passband in the flat-top transmission spectrum was measured as < 0.2 dB, which was greater by 0.1 dB compared with the theoretical result.

#88023 - $15.00 USD Received 28 Sep 2007; revised 25 Dec 2007; accepted 26 Dec 2007; published 10 Mar 2008

Disagreement in the number of side-lobe peak and the intensity difference between pass-band peak and side-lobe one results from relatively low absolute accuracy (±1.5°) of the orientation angle of the HWP. This problem can be solved by employing the HWP with more high absolute accuracy (at least ±0.2°).

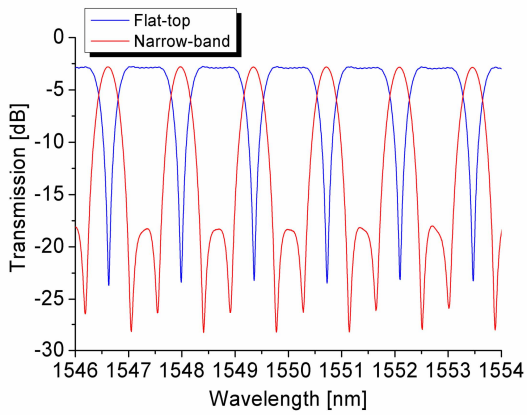

Fig. 3. Measured flat-top (blue line) and narrow-band (red line) transmission spectra of the proposed filter.

In order to compare passband bandwidths of the proposed filter with those of the conventional SBF [1], both 1 and 3 dB passband bandwidths were measured with respect to both the proposed filter (in case of flat-top and narrow-band operations) and conventional SBF constructed for comparison, as shown in Table 1. The fabricated conventional SBF was composed of a 3 dB fiber coupler, two quarter-wave plates, and 4.41 m-long Panda type PMF (birefringence: $\sim 3.98\times10^{-4}$) which is determined so that the channel separation should be ~1.37 nm (same as that of the proposed filter). Insertion loss and channel isolation of the conventional SBF were measured as ~ 1.2 dB and > 20 dB, respectively. For convenience, a figure of merit (FOM) was defined as (FOM = the bandwidth of the proposed filter [nm] / the bandwidth of the conventional SBF [nm]). Measured 1 and 3 dB bandwidths and experimental FOM's calculated based on the above definition are shown in Table 1, also including theoretical FOM's in order to estimate the deviation of the experimental results from theoretical ones. As a result, 1 and 3 dB experimental FOM's of the proposed filter in flat-top and narrow-band operations were greater by ~102.9 and 44.3 % and smaller by ~47.9 and 47.1 % than those of the conventional SBF (always one according to the definition), respectively. In particular, these results mean that 1 and 3 dB bandwidths of the proposed filter in the flat-top operation were broadened by 81.2 and 62.9 %, respectively, compared with those of the first-order PDLC filter [9]. Compared with the theoretical FOM's, the maximum deviation of experimental FOM's of the proposed filter was less than 2.9 %.

Table 1. Measured 1 and 3 dB passband bandwidths and their corresponding FOM's

	Measured bandwidth [nm]		Experimental FOM		Theoretical FOM	
	1 dB	3 dB	1 dB	3 dB	1 dB	3 dB
Flat-top operation	0.8418	1.0081	2.0289	1.4428	2.0894	1.4850
Narrow-band operation	0.2162	0.3693	0.5211	0.5286	0.5067	0.5153
Conventional SBF	0.4149	0.6987				

#88023 - $15.00 USD Received 28 Sep 2007; revised 25 Dec 2007; accepted 26 Dec 2007; published 10 Mar 2008

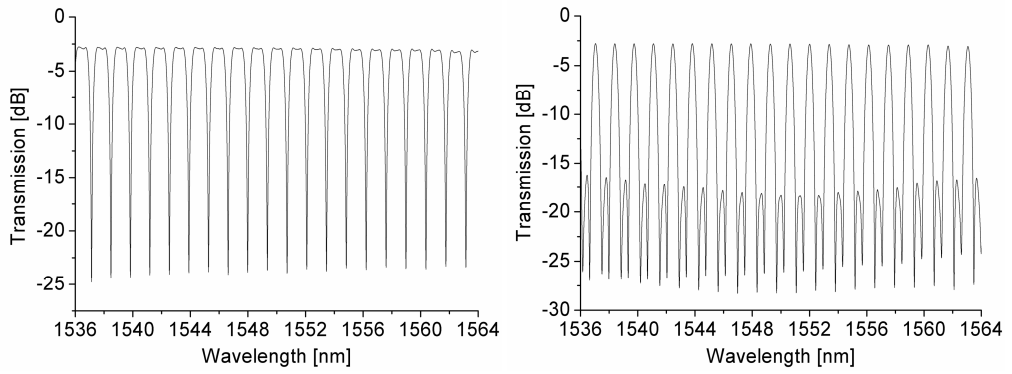

Fig. 4. Measured (a) flat-top and (b) narrow-band transmission spectra in a wide range of wavelength (28 nm).

Figures 4(a) and 4(b) show the measured flat-top and narrow-band transmission spectra at a broad wavelength range of 28 nm, respectively. The typical channel isolation of the flat-top transmission spectrum and side-mode suppression ratio of the narrow-band one were measured as > 20 and 15 dB, respectively. The spectral flatness among other transmission channels was measured as < 0.15 dB in both transmission spectra (flat-top and narrow-band spectra). Insertion loss was measured as ~2.9 dB. This mainly comes from the insertion loss of two waveplates (~0.8 dB), PBS (~1.8 dB considering a roundtrip loss), and fusion splicing loss (~0.3 dB) between two PMF's and between the PMF and SMF pigtailed from the waveplates. Input polarization independence was also experimentally verified, and the maximum polarization sensitivity was measured as < 0.5 dB, which could be affected by polarization sensitivity of a photodetector and imperfection of the PBS used in the experiments. The asymmetric peaks within passbands in Fig. 4(a) and asymmetric side lobes in Fig. 4(b) are believed to be caused by inaccuracy in the alignment of the principal axes of the PMF's, disagreement of the phase retardation differences (Γ's) among three PMF's, and wavelength dependency of the phase retardation difference (set as π at the wavelength of 1550 nm) of the HWP's used in the experiments. This spectral asymmetry can be reduced by improving the splicing technique for the alignment of the principal axes of the PMF's and employing an achromatic HWP designed for a specific wavelength range. For the passband switching or wavelength tuning of the proposed filter, various methods can be incorporated including the thermal or mechanical modulation of the PMF birefringence [12], substitution of a conventional differential delay line (birefringence modulator) for the PMF [4], and control of additional waveplates inserted between the PMF's [13].

4. Conclusion

The polarization-independent second-order all-fiber comb filter using the PDLC was embodied by the arrangement of three PMF loops and adjustment of two HWP's based on the Solc type BC. The effect of the second-order structure of the PMF loops on the bandwidth of the filter passband was theoretically investigated and experimentally demonstrated. In the implemented filter, flat-top and narrow-band transmission spectra could be obtained by the proper adjustment of two HWP's, and 1 and 3 dB bandwidths of the filter in flat-top and narrow-band operations were greater by ~102.9 and 44.3 % and smaller by ~47.9 and 47.1 % than those of the conventional SBF, respectively.

Acknowledgments

The present research was financially supported by the "High Risk High Return Project" of ETRI.

#88023 - $15.00 USD Received 28 Sep 2007; revised 25 Dec 2007; accepted 26 Dec 2007; published 10 Mar 2008